Mon. Not. R. astr. Soc. (1989) **241**, 403–413

Refractive radio scintillation in the solar wind

Ramesh Narayan *Steward Observatory, University of Arizona, Tucson, AZ 85721, USA*

K. R. Anantharamaiah* and T. J. Cornwell *National Radio Astronomy Observatory,† Socorro, NM 87801, USA*

Accepted 1989 May 2. Received 1989 May 2; in original form 1989 February 22

Summary. We have observed the strong radio source 3C279 with the Very Large Array radio interferometer when the source was at a solar elongation of 0°.9. The visibilities were measured with a time resolution of 6.67 s. We find convincing evidence for slow variations in the flux, which we interpret as refractive scintillation caused by large-scale density inhomogeneities in the solar wind. Furthermore, we find that the angular size of the scatter-broadened image of 3C279 fluctuates in a correlated fashion with the flux. This effect, which had been predicted theoretically, is verified here for the first time.

1 Introduction

Scintillation is the phenomenon by which the flux received from an intrinsically steady source varies as a result of scattering in an inhomogeneous medium between the source and the observer. Astronomical radio sources display three kinds of scintillation: (i) scattering in the interstellar medium causes Inter-Stellar Scintillation (ISS), (ii) scattering in the solar wind causes Inter-Planetary Scintillation (IPS) and (iii) scattering in the Earth's ionosphere causes Ionospheric Scintillation. ISS and IPS in particular have made significant contributions to our understanding of density fluctuations in the respective scattering media.

In a landmark paper, Rickett, Coles & Bourgois (1984), following earlier work by Shapirovskaya (1978) and Sieber (1982), brought the attention of the ISS community to a new kind of scintillation, called 'refractive' scintillation, that has a much longer time-scale (~ weeks to years) than the previously well-known 'diffractive' scintillation (time-scale ~ minutes). They showed that the puzzling low-frequency variability of compact extragalactic sources, as well as the slow variability of pulsars, is caused by this effect. Although Rickett *et al.* concentrated on ISS in their paper, refractive flux scintillation is, in fact, a more general phenomenon and is expected to occur whenever the following two conditions are satisfied:

* On leave from Raman Research Institute, Bangalore 560080, India.

† Associated Universities Inc. operates the National Radio Astronomy Observatory under National Science Foundation Cooperative Agreement No. AST-8814515.

(i) The scintillation must correspond to the regime of multi-path propagation (Scheuer 1968), which requires that the rms scattering angle $\theta_{\rm rms}$ must be $>\sqrt{\lambda/D}$, where λ is the wavelength of the radiation and D is an effective distance from the observer to the scatterers. (We refer to $\sqrt{\lambda/D}$ as the Fresnel angle since it is the Fresnel length, $l_{\rm F}\equiv\sqrt{\lambda D}$, divided by D.) Indeed, refractive scintillation becomes distinct from the usual diffractive scintillation, and separately observable, only when $\theta_{\rm rms}\gg\sqrt{\lambda/D}$. We will refer to this as the regime of 'strong scattering'. ISS corresponds to strong scattering under most observing conditions. IPS generally corresponds to weak scattering but enters the strong scattering regime at sufficiently low solar elongations (e.g. Readhead, Kemp & Hewish 1978).

(ii) The density fluctuations in the scattering medium must have power on 'refractive' lengthscales $\sim\theta_{\rm rms}D$. This condition is satisfied in both ISS and IPS since the density fluctuations appear to be caused by turbulent energy cascading across several decades of lengthscales.

The motivation of this paper is two-fold. First, the above discussion suggests that a refractive component of flux variations ought to be seen in radio sources whose lines-of-sight pass close to the Sun. Such slow scintillation has not been confirmed so far, though there have been other indications of variability due to the influence of large-scale inhomogeneities in the solar wind (e.g. Cole & Slee 1980; Gapper & Hewish 1981). We describe here observations we have made of the strong radio source 3C279 at a time when it was within a degree of the Sun and we present evidence for refractive flux variations in the data.

Secondly, Blandford & Narayan (1985) showed theoretically that, in addition to refractive flux variations, there should also be fluctuations in the angular size of the image of the scintillating source; moreover, the size fluctuations should correlate with the flux variations. These predictions have not been confirmed so far. It is hard to carry out the observations with ISS since, in most cases, the scatter-broadened image cannot be resolved even with VLBI. Also, the refractive time-scale is often several years. These limitations are removed in the case of IPS and we present here the first convincing proof that flux and angular size variations do indeed correlate in refractive scintillation.

The observations are described in Section 2 and the data analysis, including the results of our tests for refractive scintillation, is presented in Section 3. Section 4 discusses possible future applications of such observations. A complication in the case of IPS close to the Sun is that the scattering is anisotropic, leading to an elliptical scattering disc. Most previous discussions of refractive scintillation assume isotropic scattering. We present the necessary generalization in Appendices A and B.

2 Observations

The compact extragalactic radio source 3C279 was observed on several days in 1987 October with the Very Large Array (VLA) radio interferometer. At the maximum VLA angular resolution of 0.4 arcsec at λ6 cm, the source is dominated by an unresolved compact core, which has a flux density of 10.6 Jy (de Pater & Perley 1983). The jet and other compact components associated with the source are only $\sim$0.5 per cent of the peak. Therefore, for the purpose of these observations, this source can be considered as essentially unresolved.

The observations were conducted in the A-configuration of the VLA as part of an investigation of the speckle phenomenon in radio scattering (Cornwell, Anantharamaiah & Narayan 1988, 1989), but some of the data are well suited for the tests described in this paper. The best data were obtained at 6.14-cm wavelength (observing frequency 4885 MHz) on October 7, when the solar elongation of 3C279 was $e=0\overset{\circ}{.}9$. The data were recorded from one

IF pair with dual polarization with an integration of 6.67 s and using a bandwidth of 50 MHz. In all, nine minutes of data were recorded on the source. The amplitudes were calibrated using the source 3C286, assuming its flux density to be 7.41 Jy. The instrumental phases were calibrated using observations of the source 1252+119, made just before and just after the observations of 3C279. Some of the interferometers with short spacings showed anomalously high correlations due to the proximity of the Sun. These were removed from the final data set.

Further processing of the data was carried out using the Astronomical Image Processing System (AIPS). Atmospheric phase variations were corrected using self-calibration procedures (Cornwell 1985) with an integration time of 60 s. The final deconvolved image (made with the self-calibrated data) is shown in Fig. 1. The rms noise in this image is 1.5 mJy/beam and the angular resolution is 0.44×0.40 arcsec^2. The peak brightness is 198 mJy/beam, compared to 10.6 mJy/beam when the source is far away from the Sun. The signal-to-noise ratio in this

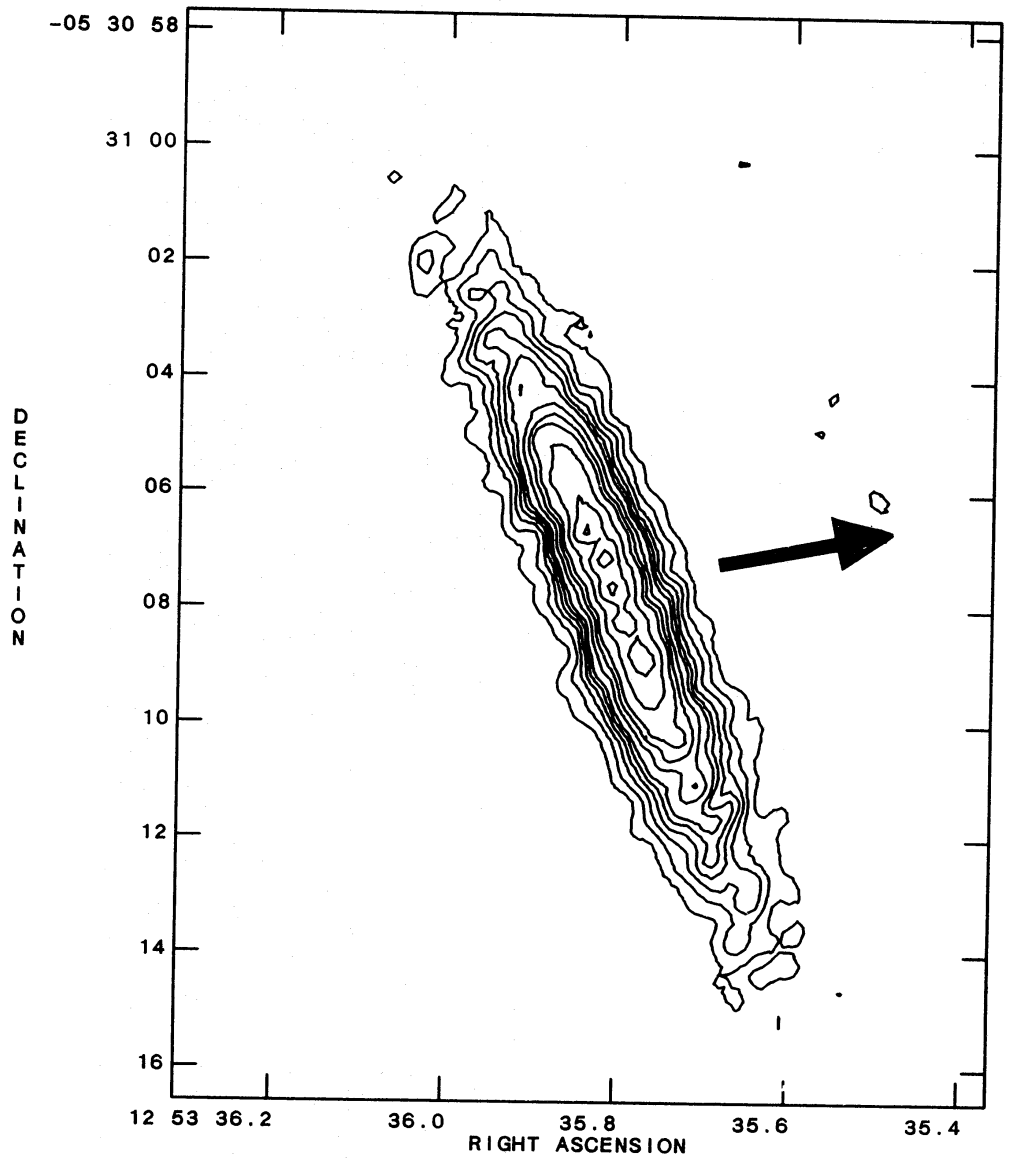

Figure 1. Image of 3C279 at $\lambda 6$ cm observed on 1987 October 7, when the solar elongation was $e = 0.^{\circ}9$. The arrow indicates the direction toward the centre of the Sun. The integration time is 9 min and the angular resolution is 0.44×0.40 arcsec^2. With 1 unit = 1.5 mJy/beam, the contour intervals are -5, 5, 10, 15, 20, 25, 30, 40, 50, 60, 80, 100, 120 and 140 units. The peak flux in the image is 198 mJy/beam.

image is ~150 and, therefore, it is not sensitive to other components in the source, which are ~0.5 per cent of the peak. (Since the weaker components are also compact, their peak flux density will be reduced by a similar factor due to scattering.)

3 Data analysis

3.1 SHAPE OF THE ENSEMBLE-AVERAGE IMAGE

From the image of 3C279 shown in Fig. 1 we reach the following conclusions:

(i) The image is strongly anisotropic (axis ratio ~6:1), which implies that the scattering is itself anisotropic, as was first noted by Hewish (1958), and confirmed more recently by Armstrong *et al.* (1986). The scattering theory for an anisotropic medium is not very well developed. Some relevant results are discussed in Appendices A and B.

(ii) The half-width of the image along its major axis is $\theta \sim 3.5$ arcsec, which corresponds to a characteristic refractive time-scale (half-width of the flux correlation function), $t_{\rm ref} \sim \theta D/v \sim (25/v_{100})$ s, where v_{100} is the velocity of the solar wind in units of 100 km s^{-1} and $D = 1$ AU. The observations extend over a time ~500 s which is greater than $t_{\rm ref}$, and so the image in Fig. 1 approaches the *ensemble-average* limit (e.g. Goodman & Narayan 1988; Narayan & Goodman 1989). The limit is achieved only approximately since there are at most two or three 'periods' of refractive flux variations (Fig. 2). Nevertheless, we feel that the results of Appendix A may be applied.

(iii) The Fresnel angle is $\sqrt{\lambda/D} = 0.13$ arcsec. Since this is much smaller than the size of the image, the observations do correspond to the strong scattering regime and refractive effects are expected to be present.

Equation (A2) in Appendix A gives the theoretically derived form of the visibilities of the ensemble-average scatter-broadening image of a point source for a power-law spectrum of phase fluctuations. We have carried out a least-squares fit of the measured visibilities to a model of this form. There are seven parameters in the model: the flux F, the orientation ϕ of

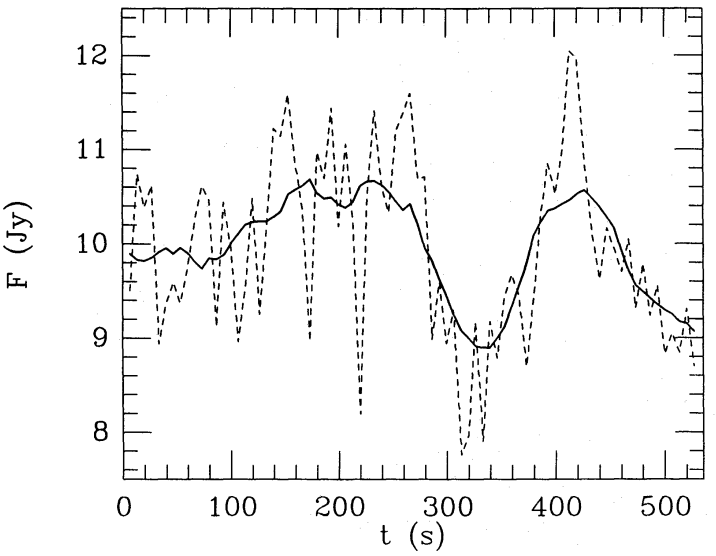

Figure 2. The dashed line shows the flux of 3C279 measured every 6.67 s. The solid line is obtained by low-pass filtering the measurements with a Gaussian filter of FWHM = 26.67 s. We interpret the flux variations in the filtered data to be evidence of refractive scintillation.

the major axis of the image, the scaling lengths x_0 and y_0, the spectral index α, and the two coordinates of the image centroid. By including parameters for the position of the image, we are directly able to fit the complex measured visibilities rather than just the moduli of the visibilities. We believe this to be the correct procedure. The results of the fit are

$$F = 10.5 \pm 0.3 \text{ Jy}, \phi = -22\overset{\circ}{.}7 \pm 0\overset{\circ}{.}3, x_0 = 4.9 \pm 0.2 \text{ km}, y_0 = 0.78 \pm 0.02 \text{ km}, \alpha = 1.41 \pm 0.05. \quad (1)$$

Formal standard deviations of the parameters are indicated, based on the assumption of random noise in the measurements.

The anisotropy of the image is given by $x_0/y_0 = 6.25$, confirming the large anisotropy found in Fig. 1. The orientation of the image indicates that the scattering blobs in the solar wind are elongated approximately radially, presumably stretched out by the solar wind flow or by the solar magnetic field. This is consistent with the results of Hewish (1958) and Armstrong *et al.* (1986). The orientation is, however, not precisely radial, but is rotated by ~ 13° such that the elongated blobs are tilted away from the rotation axis towards the solar equator. If the scatterers are stretched parallel to the projected field lines, then the sense of the tilt is consistent with a dipole field.

The value we determine for the index α differs significantly from the value of $\frac{5}{3}$ expected for Kolmogorov turbulence. This confirms earlier claims that the spectrum is shallower than Kolmogorov close to the Sun (e.g. Woo & Armstrong 1979; Harmon & Coles 1983). An interesting point is that the measurement of a value of α other than 2 implies that the inner scale of the turbulence is smaller than the linear size of the VLA (~ 10 km), since otherwise the image would have a Gaussian profile (e.g. see Narayan 1988). Assuming that the error estimate in equation (1) is representative of the true error (i.e. assuming that there are no large systematic errors), these conclusions are quite robust.

3.2 REFRACTIVE SCINTILLATION

Since the visibilities were collected once every 6.67 s, it was possible for us to measure variations in the flux of the source on this time-scale. We took the visibilities corresponding to each 6.67-s data set and carried out a model-fit along the lines described in the previous section, except that we constrained α in each case to the above best-fit estimate, $\alpha = 1.4$. This constraint was introduced because the individual 6.67-s data tended to be more noisy than the full data set and were not good enough to give independent estimates of α.

The dashed line in Fig. 2 shows the variation of F with time over the course of the observations. There appear to be two kinds of variability – a fast variability on a time-scale shorter than or comparable to the sampling and a slower variability with a 'period' of ~ 200 s (or $1/e$ half-width of $t_{1/e} \sim 30$ s). The amplitude of the fast variability seems to be too large to be consistent with noise; we ignore this variation here and discuss possible causes in Section 4. The solid line in Fig. 2 shows the result of filtering the flux variation with a Gaussian low-pass filter of FWHM equal to 26.67 s. This highlights the slow variations in the flux. We are convinced that this variation is not due to any systematic error in the observations but that it represents true refractive scintillation. To our knowledge this is the first demonstration of refractive flux scintillation in IPS. The rms variation in the smoothed flux is found to be 5.2 per cent while the theoretically predicted value for $\alpha = 1.4$ is 3.4 per cent (equation B3 in Appendix B).

The detection of refractive scintillation implies that there are density inhomogeneities in the solar wind on the scale of the projected size of the image, namely $\theta D \sim 2500$ km. We have already seen in Section 3.1 that there are density fluctuations on scales of 10 km or less. Thus,

if the density fluctuations in the solar wind are produced by a turbulent cascade, then even as close to the Sun as $e = 0.9$, the turbulence spectrum extends over more than three decades of spatial scale. The spectral index α is, however, different from the standard Kolmogorov value of $\frac{5}{3}$. A similar result was obtained by Woo & Armstrong (1979).

Although our observations appear to confirm the existence of an extended turbulence spectrum in the solar wind, it should be noted that the interpretation is not unique. For instance, the scattering model proposed by Fiedler *et al.* (1987) for the interstellar medium can also be made to work. In this case, one assumes that the medium consists of only small-scale inhomogeneities, but that their number density varies on a characteristic lengthscale. If this lengthscale is $\lesssim \theta_{\rm rms}$, then we will have slow correlated variations in the flux and angular size, as observed. In this picture, one eliminates the need for an extended density spectrum but is forced to introduce a second lengthscale in the medium.

3.3 FLUX-ANGULAR SIZE CORRELATIONS

Along with the flux, F, we also obtain the parameter y_0 for each 6.67-s dataset. Equation (A9) then allows us to estimate the FWHM angular size of the image along its major axis, $\theta_{\rm maj}$. Fig. 3 shows the low-pass filtered $\theta_{\rm maj}$ obtained from fitting the visibilities and compares the results with the variation of F. It is immediately apparent that there is a strong correlation between the two parameters. Fig. 4 plots the unfiltered F and $\theta_{\rm maj}$ values and confirms the correlation. This effect was predicted by Blandford & Narayan (1985), but had not been experimentally confirmed before.

From the data we can calculate a normalized correlation coefficient, $\langle \delta F \delta \theta_{\rm maj} \rangle / [\langle \delta F^2 \rangle \langle \delta \theta^2_{\rm maj} \rangle]^{1/2}$. The measurements give 0.68, compared to the theoretical value of 0.52 (Appendix B).

4 Discussion

The chief motivation of the present work was to detect refractive scintillation in IPS and to confirm that flux variations are correlated with fluctuations in the angular size of the image. In

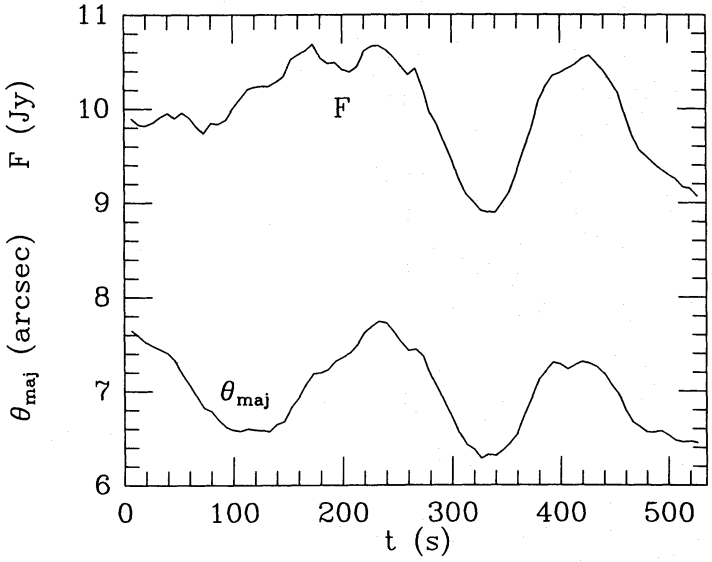

Figure 3. The line marked F is the low-pass filtered flux (Jy) of 3C279. The line marked $\theta_{\rm maj}$ is the low-pass filtered FWHM angular size of the image along its major axis. The strong correlation between F and $\theta_{\rm maj}$ confirms the prediction of Blandford & Narayan (1985).

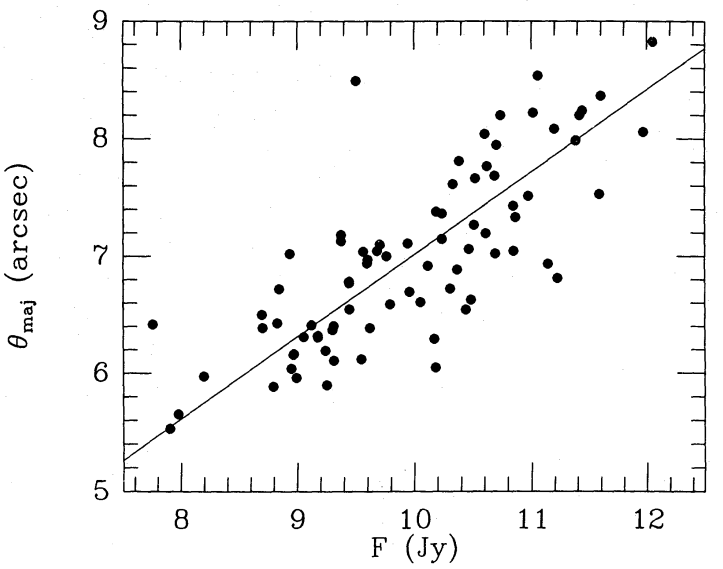

Figure 4. The points show the unfiltered θ_{maj} and F values. The straight line corresponds to a direct proportionality between θ_{maj} and F, as expected theoretically.

this we have succeeded, as shown by Figs 2–4. The quantitative agreement is moderately good, but the observed effects tend to be somewhat stronger than predicted by theory. A likely reason for this is that we have modelled the spectrum of density fluctuations as a single power-law (equation A4) whereas the index α may in reality vary with wave-vector q. In particular, if α were to increase at larger scales (lengthscales $\sim \theta D$), the observed magnitude of refractive effects could be explained without affecting the fit of the ensemble-average visibilities discussed in Section 3.1. Coles & Harmon (1988) have proposed a model spectrum of this form near the Sun, and Cordes & Wolsczan (1986) proposed a similar model for the interstellar medium.

One important factor we have not discussed in any detail is the *time-scale* of the refractive fluctuations, which is rather complicated when there is anisotropy in the scattering. A preliminary discussion is given by Narayan & Hubbard (1988) for the case when the anisotropy factor ρ is large compared to unity. Their results may be summarized as follows. Let the projected half-widths of the scatter-broadened image be σ_{min} and σ_{maj} along its minor and major axes, namely, the X and Y axes. The refractive scintillation pattern at the observer then has a correlation length $\sim \rho\sigma_{maj}$ along the x-axis and σ_{maj} along the y-axis. The motion of the solar wind causes the random fluctuation pattern on the ground to move, leading to scintillation. Because of the anisotropy of the scintillation pattern, the resulting scintillation time-scale depends on the direction of the velocity. The mean velocity of the solar wind is presumably mostly parallel to the long axis of the scattering blobs, i.e. parallel to the X-axis. This will give a scintillation time-scale, $t_1 \sim \rho\sigma_{maj}/V_{par} \sim (170/V_{par,100})$ s, where $V_{par,100}$ is the parallel component of the velocity expressed in units of 100 km s^{-1}. In addition, the solar wind probably also has a perpendicular component of velocity, either from uniform motion at an angle to the direction of elongation of the blobs or from random motions, which near the Sun may be comparable in magnitude to the mean velocity itself (Ekers & Little 1971; Armstrong & Woo 1981). If V_{perp} is this component of the velocity (parallel to the Y-axis), then we have a second potential time-scale, $t_2 \sim (27/V_{perp,100})$ s. These time-scales refer to the $1/e$-width of the flux correlation function. The data in Fig. 3 corresponds to a time-scale $t_{1/e} \sim 30$ s, suggesting that either $V_{par} \sim 600$ km s^{-1} or $V_{perp} \sim 100$ km s^{-1}. The second estimate appears to be more plausible at this time. However, more observations are needed, along with a better

understanding of solar wind motions, before a detailed quantitative comparison will be possible.

Fig. 2 shows that, in addition to the slow flux variation which we have studied, there is also a fast variation that is essentially uncorrelated from one measurement to the next. This is probably not due to measurement noise, which we estimate to be quite small. Also, the variability has too large an amplitude to be diffractive scintillation. It is possible that this is a second kind of refractive scintillation with a shorter time-scale than the one we considered. Indeed, in the presence of anisotropic scattering there are, in fact, two kinds of refractive scintillation. Narayan & Hubbard (1988) considered only the dominant slower mode for their application. This was acceptable because the anisotropy in that case was large ($\rho \sim 25$) and the second component can be shown to vanish in this limit. In the present situation, however, the anisotropy is more modest ($\rho \sim 6$), and it is conceivable that both kinds of refractive scintillation will be present. This requires more investigation.

Observations of the kind described here can provide a sensitive probe of the turbulence spectrum of the solar wind close to the Sun and would complement other approaches based on intensity and phase scintillation and spectral broadening (e.g. Readhead *et al.* 1978; Coles & Harmon 1988). Using an interferometer like the VLA it is possible to measure (within a fraction of an hour) the ensemble-average visibility $V(x, y)$ of a scatter-broadened image simultaneously on 351 baselines (27 antennas). By the discussion in Appendix A, this means that one measures the phase structure function $D_\Phi(x, y)$, which can be inverted to obtain the spectrum. By making such observations and carrying out the model-fitting procedure described in Section 3.1, one can probe the spectrum on scales varying from <1 to ~ 30 km, the range of baselines in the VLA. Moreover, by choosing different sources and different wavelengths, it is possible to study a range of solar elongations both in the ecliptic plane and off it.

Acknowledgments

We thank John Armstrong for useful discussions and the referee for many illuminating comments. RN was supported in part by NSF grant AST-8814725.

References

Armstrong, J. W. & Woo, R., 1981. *Astr. Astrophys.*, **103,** 415.
Armstrong, J. W., Coles, W. A., Kojima, M. & Rickett, B. J., 1986. In: *The Sun and the Heliosphere in Three Dimensions,* p. 59, ed. Marsden, R. G., Reidel, Dordrecht.
Blandford, R. & Narayan, R., 1985. *Mon. Not. R. astr. Soc.,* **213,** 591.
Cole, T. W. & Slee, O. B., 1980. *Nature,* **285,** 93.
Coles, W. A. & Harmon, J. K., 1988. In: *Radio Wave Scattering in the Interstellar Medium,* p. 87, eds Cordes, J. M., Rickett, B. J. & Backer, D. C., American Institute of Physics, New York.
Cordes, J. M. & Wolsczan, A., 1986. *Astrophys. J.,* **307,** L27.
Cornwell, T. J., 1985. In: *Synthesis Imaging,* eds Perley, R. A., Schwab, F. R. & Bridle, A. H., NRAO, Green Bank, West Virginia.
Cornwell, T. J., Anantharamaiah, K. R. & Narayan, R., 1988. In: *Radio Wave Scattering in the Interstellar Medium,* p. 59, eds Cordes, J. M., Rickett, B. J. & Backer, D. C., American Institute of Physics, New York.
Cornwell, T. J., Anantharamaiah, K. R. & Narayan, R., 1989. *J. opt. Soc. Am.,* in press.
de Pater, I. & Perley, R. A., 1983. *Astrophys. J.,* **273,** 64.
Ekers, R. D. & Little, L. T., 1971. *Astr. Astrophys.,* **10,** 310.
Fiedler, R. L., Dennison, B., Johnston, K. J. & Hewish, A., 1987. *Nature,* **326,** 675.
Gapper, G. R. & Hewish, A., 1981. *Mon. Not. R. astr. Soc.,* **197,** 209.

Goodman, J. & Narayan, R., 1988. In: *Radio Wave Scattering in the Interstellar Medium*, p. 200, eds Cordes, J. M., Rickett, B. J. & Backer, D. C., American Institute of Physics, New York.
Harmon, J. K. & Coles, W. A., 1983. *Astrophys. J.*, **270**, 748.
Hewish, A., 1958. *Mon. Not. R. astr. Soc.*, **118**, 534.
Narayan, R., 1988. In: *Radio Wave Scattering in the Interstellar Medium*, p. 17, eds Cordes, J. M., Rickett, B. J. & Backer, D. C., American Institute of Physics, New York.
Narayan, R. & Goodman, J., 1989. *Mon. Not. R. astr. Soc.*, **238**, 963.
Narayan, R. & Hubbard, W. B., 1988. *Astrophys. J.*, **325**, 503.
Readhead, A. C. S., Kemp, M. C. & Hewish, A., 1978. *Mon. Not. R. astr. Soc.*, **185**, 207.
Rickett, B. J., Coles, W. A. & Bourgois, G., 1984. *Astr. Astrophys.*, **134**, 390.
Romani, R. W., Narayan, R. & Blandford, R. D., 1986. *Mon. Not. R. astr. Soc.*, **220**, 19.
Scheuer, P. A. G., 1968. *Nature*, **218**, 920.
Shapirovskaya, N. Ya., 1978. *Soviet Astr.*, **22**, 544.
Sieber, W., 1982. *Astr. Astrophys.*, **113**, 311.
Tatarskii, V. I. & Zavorotnyi, V. U., 1980. In: *Progress in Optics, XVIII*, p. 207, ed. Wolf, E.
Woo, R. & Armstrong, J. W., 1979. *J. geophys. Res.*, **84**, 7288.

Appendix A: Anisotropic and one-dimensional scattering screens

Let us collapse the scattering medium to a thin screen at distance D from the observer, and let the source be at infinity. The plane wavefront from the source acquires an additional phase $\Phi(X, Y)$ on crossing the screen because of density fluctuations in the medium. X and Y are transverse coordinates on the screen measured on Cartesian axes which are chosen to lie along the principal axes of the anisotropic scattering distribution. Let the phase fluctuation be described by a spectrum of the form

$$Q(q_X, q_Y) = Q_0(\rho^2 q_X^2 + q_Y^2)^{-(\alpha+2)/2}, \quad \alpha \leq 2. \tag{A1}$$

Here q_X and q_Y are wave-vector components, ρ is the anisotropy parameter defined such that density blobs on the screen tend to be a factor ρ longer along the X-axis compared to the Y-axis, the index α is related to the more usual β by $\alpha = \beta - 2$ (e.g. Narayan 1988) and Q_0 is a normalizing constant that measures the overall strength of the phase fluctuations. The restriction $\alpha \leq 2$ corresponds to so-called Type A or 'shallow' spectra (e.g. Narayan 1988).

Narayan & Hubbard (1988) have studied this form of the spectrum and have worked out the ensemble-average mutual intensity or visibility, $V(x, y)$, on a baseline (x, y) for a unit point source; x and y are chosen to be parallel to X and Y. The result is

$$\langle V(x, y)\rangle = \exp\left\{-\frac{2^{-\alpha}\Gamma[(4-\alpha)/2]Q_0}{\pi(2-\alpha)\alpha\Gamma[(\alpha+2)/2]\rho}\left(\frac{x^2}{\rho^2}+y^2\right)^{\alpha/2}\right\}$$

$$\equiv \exp\left\{-\left(\frac{x^2}{x_0^2}+\frac{y^2}{y_0^2}\right)^{\alpha/2}\right\}, \tag{A2}$$

$$y_0 = \frac{x_0}{\rho} = \left\{\frac{\pi(2-\alpha)\alpha\Gamma[(\alpha+2)/2]\rho}{2^{-\alpha}\Gamma[(4-\alpha)/2]Q_0}\right\}^{1/\alpha}. \tag{A3}$$

The angle brackets on $V(x, y)$ indicate an *ensemble-average*. This limit is achieved by integrating the visibilities over a time much greater than the refractive scintillation time-scale (Goodman & Narayan 1988; Narayan & Goodman 1989). Note that, for $\rho > 1$, the visibilities fall off more slowly along the x direction than the y direction. This means that the image has a larger angular size parallel to Y than X. Thus, the image is elongated along a direction

orthogonal to the direction of elongation of the scattering blobs. The magnitude of the anisotropy in the image is the same as that of the scattering blobs.

When ρ is large, the scattering occurs almost exclusively in the Y-direction. It is then acceptable for certain purposes to ignore the scattering along X altogether and to consider a simpler problem where the spectrum of phase fluctuations is a function only of q_Y. This is equivalent to assuming that the scattering blobs are infinitely elongated along the X-direction. Let us write

$$Q(q_Y) = Q'_0 q_Y^{-(\alpha+1)}, \quad \alpha \leq 2. \tag{A4}$$

The choice of the index will become clear below. It is straightforward to calculate the phase structure function for this case (e.g. Tatarskii & Zavarotnyi 1980),

$$D_\Phi(Y) = \langle [\Phi(Y'+Y) - \Phi(Y')]^2 \rangle = \frac{Q'_0}{\pi} \int_{-\infty}^{\infty} q_Y^{-(\alpha+1)} (1 - \cos q_Y Y)\, dq_Y$$

$$= \frac{2^{1-\alpha}\Gamma[(2-\alpha)/2] Q'_0}{\sqrt{\pi}\alpha\Gamma[(\alpha+1)/2]} Y^\alpha. \tag{A5}$$

The ensemble-average visibility is then given by

$$\langle V(y) \rangle = \exp\left[-\frac{1}{2} D_\Phi(y) \right] = \exp[-(y/y_0)^\alpha], \tag{A6}$$

$$y_0 = \left\{ \frac{\sqrt{\pi}\alpha\Gamma[(\alpha+2)/2]}{2^{-\alpha}\Gamma[(2-\alpha)/2] Q'_0} \right\}^{1/\alpha}. \tag{A7}$$

The variation of $\langle V(y) \rangle$ with y in equation (A6) is the same as that of $\langle V(x, y) \rangle$ with y in equation (A2). This shows that (A4) is indeed the appropriate one-dimensional spectrum corresponding to the anisotropic spectrum (A1). The length y_0 describes a characteristic baseline at which the visibility falls to $1/e$ of the total flux.

The intensity profile of the image is obtained by Fourier transforming $\langle V(y) \rangle$. The FWHM of the image is then found to be

$$\theta_{\mathrm{FWHM}} = 0.90 \text{ arcsec} \left(\frac{\lambda}{1 \text{ cm}} \right) \left(\frac{y_0}{1 \text{ km}} \right)^{-1}. \tag{A9}$$

Following the discussion in Section 1, the strong-scattering regime corresponds to the case when $\theta_{\mathrm{FWHM}} \gg \sqrt{\lambda/D}$. This translates to the requirement

$$y_0 \ll \sqrt{\lambda D} \equiv l_F, \tag{A10}$$

where l_F is the Fresnel scale, In the present application, $y_0 = 0.78$ km (equation 1) and $l_F = 96$ km, and this condition is amply satisfied.

Appendix B: Refractive scintillation with one-dimensional scattering

Blandford & Narayan (1985, see also Romani, Narayan & Blandford 1986) used a geometrical optics approximation to develop a simplified theory of refractive scintillation. This approach enabled them to work out the magnitudes of several refractive effects. Their results are valid for an isotropic two-dimensional scattering screen in the limit of strong scattering [which

requires the condition (A10) to be valid]. Because of the highly anisotropic scattering in the present application, a better approximation is to consider a one-dimensional scattering screen. It is straightforward to carry though the analysis for this case using the spectrum given in (A4). We merely quote the relevant results here.

Let the image be approximated by a Gaussian profile of the form

$$I(\theta_y)=\exp[-D^2\theta_y^2/2\sigma^2]. \tag{B1}$$

This representation is exact for $\alpha=2$ and is adequate even for the case of interest, $\alpha=1.4$. By equating the $1/e$ point of the visibility of this profile with y_0 in equation (A6), we find

$$\sigma=D\lambda/\sqrt{2}\pi y_0. \tag{B2}$$

Let $\delta F(y)$ represent the normalized refractive fluctuation in the received flux at the point y on the observer plane. The mean square fluctuation $\langle(\delta F\ )^2\rangle$ is then given by

$$\langle(\delta F\ )^2\rangle_y=K\Gamma[(4-\alpha)/2], \tag{B3}$$

where the dimensionless parameter K is defined by

$$K=\frac{Q_0'\lambda^2L^2}{8\pi^3\sigma^{4-\alpha}}=\frac{\alpha\Gamma[(\alpha+1)/2]}{2^{3-3\alpha/2}\pi^{5/2-\alpha}\Gamma[(2-\alpha)/2]}\left(\frac{\lambda D}{\sigma^2}\right)^{2-\alpha}. \tag{B4}$$

The last relation follows from equation (A10) and (A7). For the particular observations described in this paper, $K=0.0013$. Let $\delta\theta(y)$ be the fluctuation in the angular size, normalized by the mean angular size, σ/D. The mean square fluctuation of this is found to be

$$\langle(\delta\theta)^2\rangle_y=K\left\{\Gamma[(4-\alpha)/2]-\Gamma[(6-\alpha)/2]+\Gamma[(8-\alpha)/2]/4\right\}. \tag{B5}$$

Finally, the cross-correlation between δF and $\delta\theta$ is given by

$$\langle\delta F(y)\delta\theta(y)\rangle_y=K\{\Gamma[(4-\alpha)/2]-\Gamma[(6-\alpha)/2]/2\}. \tag{B6}$$